Journal of Magnetism and Magnetic Materials 571 (2023) 170538

Contents lists available at ScienceDirect

Journal of Magnetism and Magnetic Materials

journal homepage: www.elsevier.com/locate/jmmm

An effect of magnetohydrodynamic and radiation on axisymmetric flow of non-Newtonian fluid past a porous shrinking/stretching surface

U.S. Mahabaleshwar [a,*], T. Maranna [a], L.M. Pérez [b], S.N. Ravichandra Nayakar [c]

[a] Department of Studies in Mathematics, Davangere University, Shivagangothri, Davangere 577 007, India
[b] Departamento de Física, FACI, Universidad de Tarapacá, Casilla 7D, Arica, Chile
[c] Department of Mathematics, University BDT College of Engineering, 577004 Davangere, India

ARTICLE INFO

Keywords:
MHD
Permeable medium
Mass transpiration
Radiation
Navier condition
Prandtl number

ABSTRACT

The magnetohydrodynamic axisymmetric flow of Casson fluid over a nonlinear permeable shrinking or stretched surface is discussed in this article. Indeed, the heat transfer characteristics of an axisymmetric fluid across a non-linearly shrinking or stretching surface provided by a Casson fluid are examined analytically. Thermal radiation term is incorporated into the equation for the temperature field. Through sufficient transformations, the aforementioned non-linear PDEs are turned into ODEs. The transformed equations are then solved analytically. And an incomplete gamma function is used to depict the temperature solution analytically. The temperature equation is transformed to an incomplete gamma functions using the Rosseland approximation for the radiation and solved analytically. To estimate mass transpiration analytically, the momentum equation is investigated. To acquire the analytical results, this mass transpiration is carried out in the analysis of heat transfer under the Navier slip condition. Graphical analysis can be used to assess important physical aspects like the magnetic field, Casson parameter, mass transpiration, radiation, and Prandtl number. Dual solutions for the velocity, temperature and skin friction were obtained. In fact, for higher Prandtl number, the temperature inside the boundary layer reduces. The resulting dual solution projects that local skin friction coefficient a escalates in the first branch solution and decelerates in the second branch solution with the increase in the magnetic parameter. additionally, efficiency is increased for higher values of thermal radiation.

1. Introduction

In light of the fact that magnetohydrodynamic flows are employed in engineering as well as industries through magnetohydrodynamic pumps, the mobility of ionized gases, MHD generators, and the movement of different gases with respect to the geomagnetic field, It is provided that magnetic fields have a substantial impact on the flow of electrically conductive fluids, hence, several researchers [1–4] have conducted research on the impact of a magnetic field on the motion of an electrically conductive fluid. Due to its numerous uses in various technical disciplines, the flow of boundary layers driven by a steady straightening / shrinking surface has gathered a lot of interest in the last few decades. A few examples of practical applications for moving stretched/shrinked surfaces include wire tracking, sheet and paper manufacturing, the crystallization of fluid magnificent stones, the fabrication of glass and fibre, etc. The use of the movement of boundary layers for a continuous, extended surface flowing at a constant rate was initially established by Sakiadis [5–6] in light of the aforementioned applications. Crane [7] studied the flow that occurs when a plate containing liquid at rest is entered through a slit while moving at a constant speed, both immediately and in the future. The invention of the crane has been examined from a variety of physical viewpoints and specific perspectives due to its numerous mechanical implementations. Recently, though, a study on the flow across a diminishing surface has attracted a lot of interest. The investigation of flow across a surface that is shrinking was started by Miklavcic [8]. They revealed a lack of vorticity restricted inside a barrier layer along with a constant flow that requires substantial suction at the barrier in order to exist. Since then, many studies have been conducted to examine various facets of this issue, including those by researchers [9–11], to mention a few.

Owing to its expanding applications in engineering as well as cutting-edge technology during the past several decades, flow studies in porous media have attracted researchers' attention. A mixture of fluid as well as

* Corresponding author.
E-mail addresses: u.s.m@davangereuniversity.ac.in (U.S. Mahabaleshwar), marannat4@gmail.com (T. Maranna), lperez@academicos.uta.cl (L.M. Pérez), mathsravi@gmail.com (S.N. Ravichandra Nayakar).

https://doi.org/10.1016/j.jmmm.2023.170538
Received 11 December 2022; Received in revised form 18 January 2023; Accepted 13 February 2023
Available online 16 February 2023
0304-8853/

Nomenclature

List of symbols	Definition (S.I. Units)
A	Constant (-)
B^2	Magnetic field (Tesla)
C_p	Specific heat (JK^{-1} Kg^{-1})
d	Stretching/shrinking parameter (-)
Da^{-1}	Inverse Darcy factor (-)
f	Velocity stream function (-)
f_w	Mass suction/injection (-)
K	Permeability (N/A^2)
M	Magnetic parameter (-)
N_r	Radiation factor (-)
Pr	Prandtl number (-)
T	Temperature of fluid (K)
T_w	Temperature of surface (K)
T_∞	Ambient temperature (K)
u_1, w_1	r_1, z_1 axis velocity components.(ms^{-1})
r_1, z_1	Coordinates (-)
λ	Casson parameter (-)
Γ	Navier velocity slip (-)

Greek symbol

α	Constant (-)
κ	Fluid's thermal conductivity ($Wm^{-1}K^{-1}$)
μ	Dynamic viscosity (Ns m-1)
η	Similarity variable (-)
ρ	Density (Kg/m^3)
ν	Kinematic viscosity (m^2s^{-1})
θ	Fluctuating temperature (-)
σ	Electrical conductivity of fluid (S/m)

Abbreviation

σ^*	Stefan-Boltzmann constant ($Wm^{-2}K^{-4}$)
MHD	Magnetohydrodynamic (-)
ODEs	Ordinary differential equation (-)
PDEs	Partial differential equation (-)

solids with interconnected pores which allow liquid to travel through them or across it is referenced to as porous materials. The base material is often a solid. In the context of suction/injection, Navier slip, as well as a super linear stretched sheet, the Magnetohydrodynamic movement of an electrically conducting Nanofluid flow is explored by Mahabaleshwar [12]. the linear Navier slip barrier condition-induced stable velocity with circulation of a viscoelastic fluid under radiation heat transfer in a permeable material by Mahabaleshwar [13]. For the motion of Walters' liquid B owing to permeable stretched as well as contracting with mass and heat transfer, laminar stream is used according to an effects of mass transpiration and Navier slip has been addressed by Anusha [14].

Numerous studies have been conducted on flowing boundary layers beyond stretchable sheet planer, according to a literature review [15–16], moreover, among every passing generation, axisymmetric flow as a feature across radiating extending surface is growing in importance among researchers. Ariel [17] looked at the axially symmetric flow of Newtonian water across a stretched sheet with a slight slip at the borders. With the use of HAM technique, Sajid [18] conduct work on a viscous fluid flowing axisymmetrical along non-linearly stretched surface provides the quantitative solution. Very recently, while in existence of an applied magnetic field, boundary layer Navier slip flow across stretched surface is investigated by Mahabaleshwar [19], using the DTM-Pade method to derive approximatively solutions. Soomro [20] investigated an effects of a slip stimulation on axisymmetric liquid moving through a contracting cylinder produced by mixed convection of a water-based copper nanoparticles.

Non-Newtonian fluids are being used more and more, particularly in plasma streams, mercurial amalgamation, metal catalysts as well as alloys, nuclear fuel sledges, heavier crude and lubricant flows, paper coatings, polymeric extrusion flows, and several other operations. Considering these facts, knowing non-Newtonian fluid dynamics, either with or without heat exchange, is very important for a better understanding of topics like food refrigeration and polymer infusion, among others. Due to their complicated composition and intricate interactions with the flow field, non-Newtonian fluids are typically far more problematic to research. Much knowledge of non-Newtonian fluids is extremely empirical. Non-Newtonian fluid flows are governed by extremely nonlinear equations. Numerous non-Newtonian manufacturing fluids Some fluids exhibit solid-like elastic behavior, with Shear stress formation is a part of the governing equations for such liquids. Casson fluid is one of these fluids that is not Newtonian. Therefore, flow can occur if the shear force is greater than the shear stress. Abbas [21] investigated the effects of a dual chemical reaction, activation energy, and stretching and shrinking a sheet around a stagnation point in a non-Newtonian Casson liquid incorporating thermal radiation. Axisymmetric Magnetohydrodynamic Casson fluid flow beyond a rotating cylinder is studied by Javed [22]. The cylinder's torsional movement is what essentially causes the flow. It has been described how heat radiation as well as velocity slip affect the movement of MHD Casson liquid past an extended sheet at the stagnation point by Raza [23]. The biomechanics and polymer processing industries both benefit from the use of Casson fluid; for examples, see References [24,25,26,27], and several references therein. Moreover, Heat and flow across a rotating disc due to a uniform horizontal magnetic field is studied by Turkyilmazoglu [28]. The electrically conducting compressible laminar fluid flowing on a porous rotating disc using steady magnetohydrodynamics (MHD) is analyzed by Turkyilmazoglu [29], and also conducted research [30] on flow and heat characteristics of few nanoparticles past a deformable and porous material. Recently, the mixed convection MHD flow of heat transfer stretches or contracts a nonlinear sheet of carbon nanotubes is investigated analytically by Anuar [31]. The magnetohydrodynamic hybrid $Cu\text{-}Al_2O_3$/water nanofluid flow over a permeable stretched sheet under the impact of velocity slip as well as thermal radiation is addressed by Wahid [32]. In recent studies, the effects of temperature changes on different logarithmic surfaces. Jalili [33] studies the transfer of heat in a single dimension. A new method for analyzing fractions using the time–space fractional equations found in oil pollution and Newtonian fluid with fractional differential equations is investigated by Jalili [34–35]. Moreover, some researchers [36–40] conducted a research on properties of ferrofluid, micropolar ferrofluid, hybrid nanofluid, Williamsons fluid, micropolar nanofluid flow over stretching/shrinking sheet with effect of different parameters such as magnetic field, thermal radiation, thermophoresis, Brownian motion and hall effects. Hassan [41] researched the flow and heat transfer of a fluid under shear through a non-linear stretched sheet with a variable thickness.

Furthermore, many scientists have explored different fluids, but only a few have considered non-Newtonian fluids due to the complexities that arise due to the non-linearity. The accurate treatment of the stream of Casson fluid suspended with hybrid nanoparticles together with dust particles through a stretched sheet in the presence of Lorentz force is portrayed by Khan [42]. MHD was used to investigate the Casson liquid mixed convective flow through a channel is depicted by Raza [43]. The stability of natural convection heat transfer, and convective heat

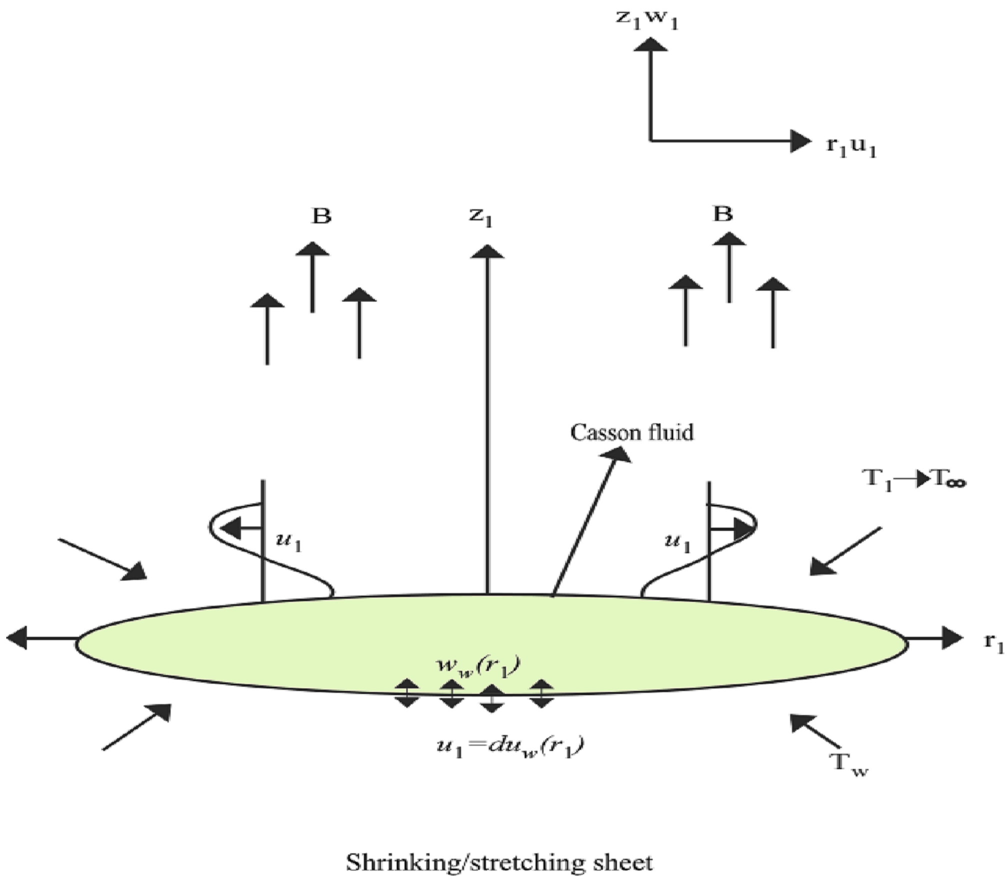

Fig. 1. Schematic representation of the flow problem.

transfer of titania nanofluids of different base fluids in a cylindrical annulus with discrete isoflux heat sources of various lengths is investigated numerically by Oudina [44–45]. Reddy [46] discusses quantitatively the effect of thermal radiation on the flow of a Williamson nanofluid through a porous material at a stretched surface while accounting for velocity and thermal slip. With the assistance of numerical solutions, Shafiq [47] analyzed the non-Newtonian Walters-B nanofluid over stretched Riga plate with Newtonian heating. Thermal Analysis of a Hybrid-Nanofluids Solar Collector and Cumulative Storage System is proposed by Dhif [48]. In another research, between two stretchable discs, a viscous, incompressible, laminar, axisymmetric flow of a micropolar fluid with the presence of a magnetic field is examined by Jalili [49].

Motivated by the abovementioned investigations, in the present work, we analyze the effect of magnetohydrodynamic and radiation on flow of axisymmetric non-Newtonian fluid over a stretching/shrinking sheet in the presence of porous medium. The governing coupled, nonlinear partial differential equations of the flow of heat and transfer problems are transferred into non-linear, coupled ordinary differential equations by using a similarity transformation. These coupled non-linear ordinary differential equations subject to the appropriate boundary conditions are solved analytically. The novelty of the present work explains that the momentum and energy equation solved analytically to get the solution domain and the expressed the solution in terms of incomplete gamma function. There are several factors considered in the present article, including radiation, the Navier-Slip impact, the magnetic parameter, mass suction/injection, and the Casson parameter. The solution curves are displayed, along with comprehensive discussions. The work is used in many industrial and engineering applications, viz., power engines, advanced nuclear systems, automobiles, biological sensors, drug delivery, and entropy generation.

2. Development of problem

Suppose a 2D steady incompressible viscous Casson fluid flow with magnetohydrodynamic boundary layers with heat transfer that is confined via a radiating penetrable non-linear stretched /diminishing surface that is exposed via radiant energy along to (r_1, ε) plane. Fig. 1 displays the flow pattern of the mathematical model associated with embedded Casson fluid and their appropriate cartesian cylindrical co-ordinates (r_1, ε, z_1). Where the r_1- axis of component is boosted within parallel plane, besides even z_1- coordinated plane is dominated within a perpendicular position, appropriately. Stream is symmetric to (r_1, ε)-plane as well as asymmetrical around the z_1 direction. Presumably, the sheet surface's modeling velocity is$u_w(r_1) = br_1^3$, while b is the arbitrarily chosen constant. Moreover, It is presumed that the magnetic force is fluctuating because $B(r_1) = r_1 B_0$ which acts parallel to the sheet's boundary. The estimated acceleration of wall mass transfer is consider as$w_w(r_1) = -r_1 v_0$, in which $w_w < 0$ and $v_0 > 0$ denote mass injection. Whereas $w_w > 0$ with $v_0 < 0$ represents mass suction.

We assume that the rheological formula for an isotropic and incompressible movement of a Casson fluid can be formulated being [50–52].

$$\tau_{ij} = \begin{cases} 2\left(\mu_B + \dfrac{p_y}{\sqrt{2\pi}}\right) e_{ij}, & \pi > \pi_c \\ 2\left(\mu_B + \dfrac{p_y}{\sqrt{2\pi}}\right) e_{ij}, & \pi < \pi_c \end{cases}, \tag{1}$$

here μ_B is the plastic dynamics viscosity of the Casson fluid, p_y is the yield stress of the fluid, π is the product of the component of deformation

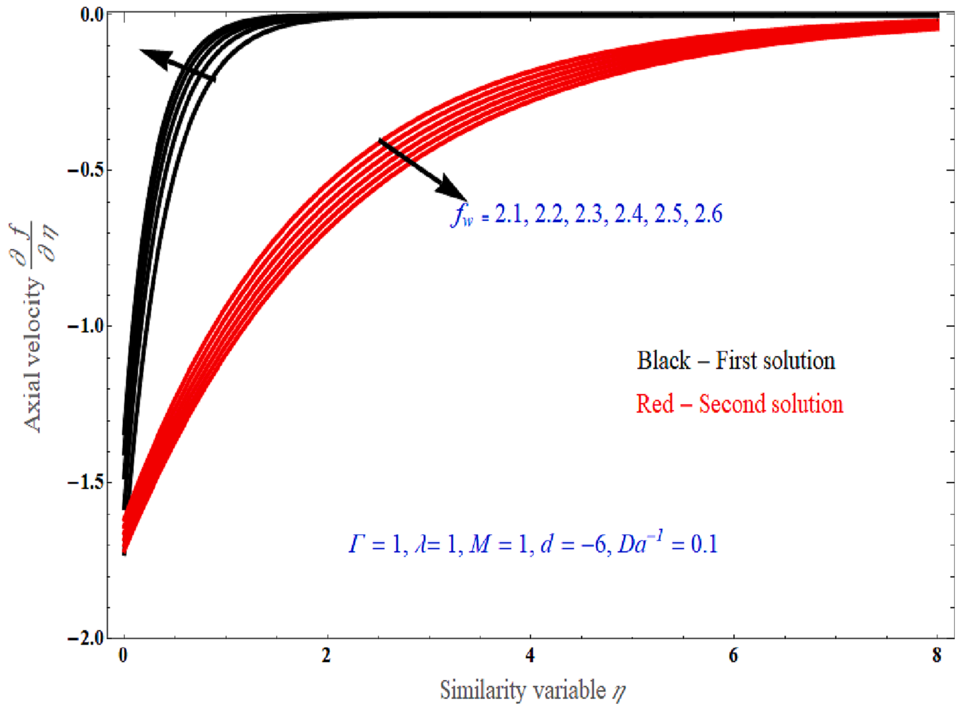

Fig. 2. An impact of f_w on velocity profile.

rate with itself, specially,$\pi = e_{ij}e_{ij}$, the deformation rate $(i,j)^{\text{th}}$ component is callede_{ij}. While π_c is the critical value of the product of the component of the deformation rate with itself. In light of these presumptions, the steady-state fundamental regulating expression for this problem can be designated as cylindrical coordinates in Cartesian space (r_1, ε, z_1), which are written as follows [57]:

$$\frac{\partial u}{\partial r_1} + \frac{u_1}{r_1} + \frac{\partial w_1}{\partial z_1} = 0, \tag{2}$$

$$u_1\frac{\partial u_1}{\partial r_1} + w_1\frac{\partial u_1}{\partial z_1} = \left(1 + \frac{1}{\lambda}\right)\nu\frac{\partial^2 u}{\partial z_1^2} - \frac{\nu}{K}u_1 - \frac{\sigma B^2(r_1)}{\rho}u_1, \tag{3}$$

$$u_1\frac{\partial T_1}{\partial r_1} + w_1\frac{\partial T_1}{\partial z_1} = \frac{\kappa}{\rho C_p}\frac{\partial^2 T_1}{\partial z_1^2} - \frac{1}{\rho C_p}\frac{\partial q_r}{\partial z_1}, \tag{4}$$

Imposed boundary constraints [57,58] for the equations (2) -(4).

$$u_1 = du_w(r_1) + A\frac{\partial u_1}{\partial z_1}, \quad w_1 = w_w(r_1), \quad T_1 = T_w, \quad \text{at } z_1 = 0, \\ u_1 \to 0, \quad T_1 \to T_\infty, \quad \text{as } z_1 \to \infty. \tag{5}$$

where (u_1, w_1) are the components of velocities along (r_1, z_1) axis respectively, the fluid kinematic viscosity is known to beν, σ be the electrical conductance of fluid, Density of the fluid is denoted asρ, κ is called as thermal conductivity of fluid, where d be the shrinking/stretching factor, A is the first order slip component, K is the permeability of the porous medium, λ is the casson parameter, σ is the electrical conductivity of the fluid,B is the external magnetic field variable,ρC_p is the specific heat capacitance of the fluid and description of other parameters are mentioned in the nomenclature part this paper.

The following proper self-similarity transformations were recommended to facilitate the analysis of the problem.

$$\eta = \sqrt{\frac{\alpha}{\nu}}z_1 r_1, \quad \theta(\eta) = \frac{T_1 - T_\infty}{T_w - T_\infty}, \quad \psi = \sqrt{\alpha\nu}r_1^3 F(\eta), \tag{6}$$

Presently ψ be the respective stream function. Additionally, demonstrate ψ using its constituent parts as $u_1 = \frac{1}{r_1}\frac{\partial\psi}{\partial z_1}$ with$w_1 = -\frac{1}{r_1}\frac{\partial\psi}{\partial r_1}$. Finally, use Eqn. (6) to these equations to obtain the velocities in the format shown below:

$$u_1 = \alpha r_1^3 F'(\eta) w_1 = -\sqrt{\alpha\nu}r_1(3F(\eta) + \eta F'(\eta)) \tag{7}$$

The radiative heat flux q_r can be determined using the Rosseland approach [53–56].

$$q_r = -\frac{4\sigma^*}{3k^*}\frac{\partial T^4}{\partial z_1}, \tag{8}$$

where σ^* is the Stephen Boltzmann constant and k^* is the mean absorption coefficient respectively. Interestingly, by employing the Rosseland approximation, on expanding T^4 in the form of Taylor series and ignoring the higher order terms to get,

$$T^4 \cong 4T_\infty^3 T - 3T_\infty^4, \tag{9}$$

The radiation term in equation (4) then implies the following form.

$$\frac{\partial q_r}{\partial z_1} = \frac{16\sigma^*}{3k^*}\frac{\partial^2 T_1}{\partial z_1} \tag{10}$$

Invoking equation (10), equation (4) gets modified [35–36] as.

$$u_1\frac{\partial T_1}{\partial r_1} + w_1\frac{\partial T_1}{\partial z_1} = \left(\frac{\kappa}{(\rho C_p)} + \frac{16\sigma^* T_\infty^3}{3k^*(\rho C_p)}\right)\frac{\partial^2 T}{\partial z_1^2}, \tag{11}$$

In the view of similarity transformations mentioned above, equations (2) -(4) simplify to.

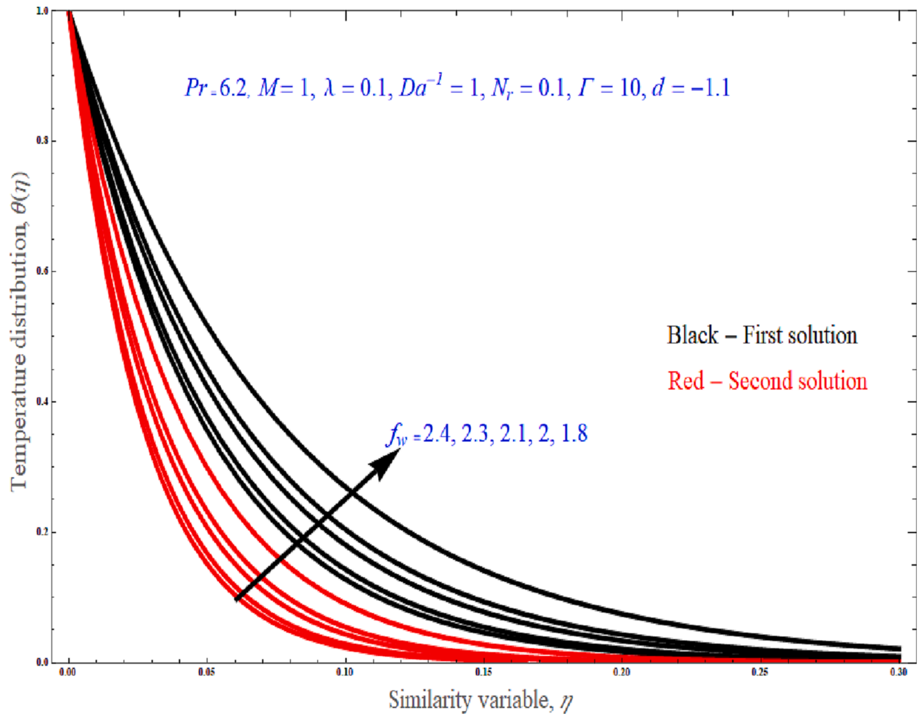

Fig. 3. An impact of f_w on temperature profile.

$$\left(1+\frac{1}{\lambda}\right)\frac{d^3F}{d\eta^3}+3F(\eta)\frac{d^2F}{d\eta^2}-3\left(\frac{dF}{d\eta}\right)^2-\left(Da^{-1}+M\right)\frac{dF}{d\eta}=0, \tag{12}$$

$$(1+N_r)\frac{d^2\theta}{d\eta^2}+3PrF(\eta)\frac{d\theta}{d\eta}=0, \tag{13}$$

In which λ is to be Casson parameter, inverse Darcy number is denoted by $Da^{-1}=\frac{\nu}{K\alpha}$, $M=\frac{\sigma B_0^2}{\rho\alpha}$ is the magnetic parameter, Prandtl number is Pr, together with radiation parameter is defined by $N_r=\frac{16\sigma^* T_\infty^3}{3k^* k(\rho C_p)}$.

The corresponding modified boundary conditions are.

$$\frac{dF}{d\eta}=d+\Gamma\frac{d^2F}{d\eta^2},\quad F(\eta)=f_w,\quad \theta(\eta)=0,\quad \text{at}\ \eta=0,$$
$$\frac{dF}{d\eta}\to 0,\quad \theta(\eta)\to 0,\quad \text{as}\ \eta\to\infty. \tag{14}$$

where d represents the shrinking/stretching factor, besides $\Gamma=$

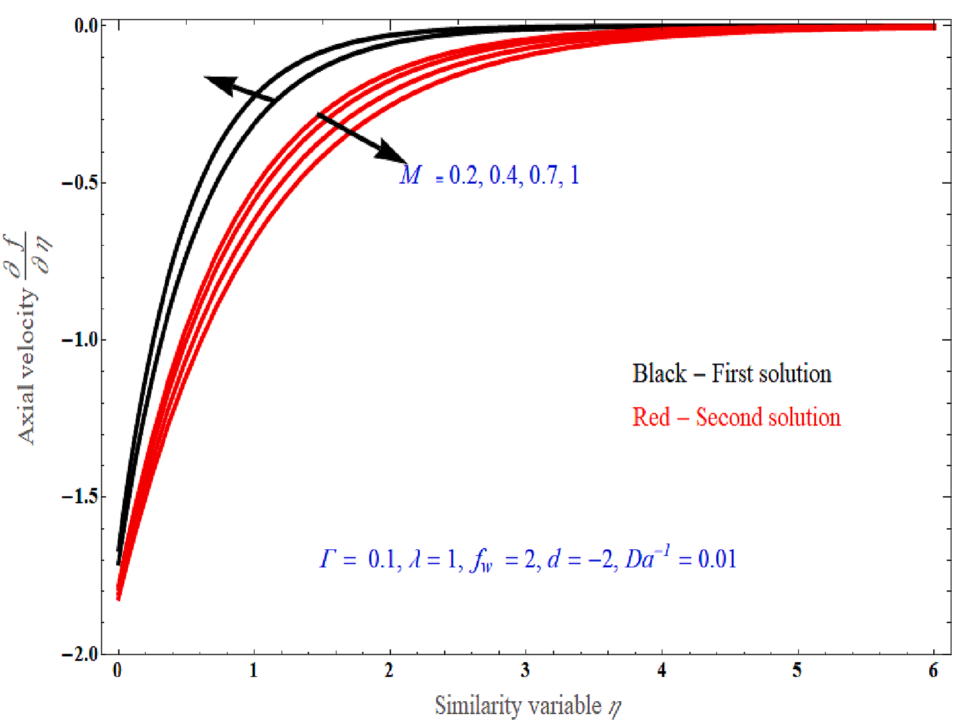

Fig. 4. An impact of M on velocity profile.

$Ar_1\sqrt{\frac{\alpha}{\nu}}$ is the Navier first order slip. Coefficient mass transfer is designated asf_w, among $f_w > 0$ for suction and $f_w < 0$ for injection.

2.1. Physical quantities of interest

The non - dimensional skin friction factor, which is the physical quantity of interest, is characterized as.

$$C_f = \frac{2\mu}{\rho}\left(\frac{\partial u_1}{\partial z_1}\right)_{z_1=0}, \tag{15}$$

and using the similarity variable, we obtain the following value for the local skin friction coefficient:

$$0.5Re_{r_1}^{\frac{1}{2}}C_f = \left(\frac{d^2f}{d\eta^2}\right)_{\eta=0} \tag{16}$$

where$Re_{r_1} = \frac{u_w(r_1)r_1}{\nu}$, is the Reynolds number.

3. Analytical solution

This part of the report demonstrates the operations of the analytical solution methodology. We must obtain the closed-form exact solutions to equation (12) as well as equation (13) in the given problem, consistent to the appropriate boundary conditions (14). Consequently, bearing in mind the method of comparing earlier work [57]. Under the condition of boundary conditions (14), we obtain the analytical or exact solution of equation (12) in the procedure outlined below:

$$F(\eta) = f_w + \frac{d}{\delta(1+\Gamma\delta)}(1-e^{-\delta\eta}), \tag{17}$$

With.

$$\frac{dF}{d\eta} = \frac{d}{(1+\Gamma\delta)}e^{-\delta\eta}, \tag{18}$$

in order to substitute equations (17–18), second and third derivative of $F(\eta)$ in equation (12), we obtain cubic polynomial in terms ofδ.

$$\left(1+\frac{1}{\lambda}\right)\Gamma\delta^3 + \left\{\left(1+\frac{1}{\lambda}\right) - 3f_w\Gamma\right\}\delta^2 - \left(3f_w + \Gamma Da^{-1} + M\Gamma\right)\delta - \left(3d + Da^{-1} + M\right) = 0, \tag{19}$$

which provides one real roots along with one pair of conjugate complex roots.

equation (19) can be rewrite as.

$$\xi_1\delta^3 + \xi_2\delta^2 - \xi_3\delta + \xi_4 = 0, \tag{20}$$

roots of the above equation (20) is expressed as.

$$\delta_1 = -\frac{\xi_2}{3\xi_1} - \frac{2^{\frac{1}{3}}(-\xi_2^2 - 3\xi_1\xi_3)}{3\xi_1 m_1} + \frac{m_1}{3*2^{\frac{1}{3}}\xi_1},$$

$$\delta_{2,3} = -\frac{\xi_2}{3\xi_1} + \frac{(1\pm i\sqrt{3})(-\xi_2^2 - 3\xi_1\xi_3)}{3*2^{\frac{2}{3}}\xi_1 m_1} - \frac{(1\mp i\sqrt{3})m_1}{6*2^{\frac{1}{3}}\xi_1}. \tag{21}$$

where.

$$m_1 = \left(-2\xi_2^3 - 9\xi_1\xi_2\xi_3 + 27\xi_1^2\xi_4 + \sqrt{4\left(-\xi_2^2 - 3\xi_1\xi_3\right)^3 + \left(-2\xi_2^3 - 9\xi_1\xi_2\xi_3 + 27\xi_1^2\xi\right)^2}\right)^{\frac{1}{3}},$$

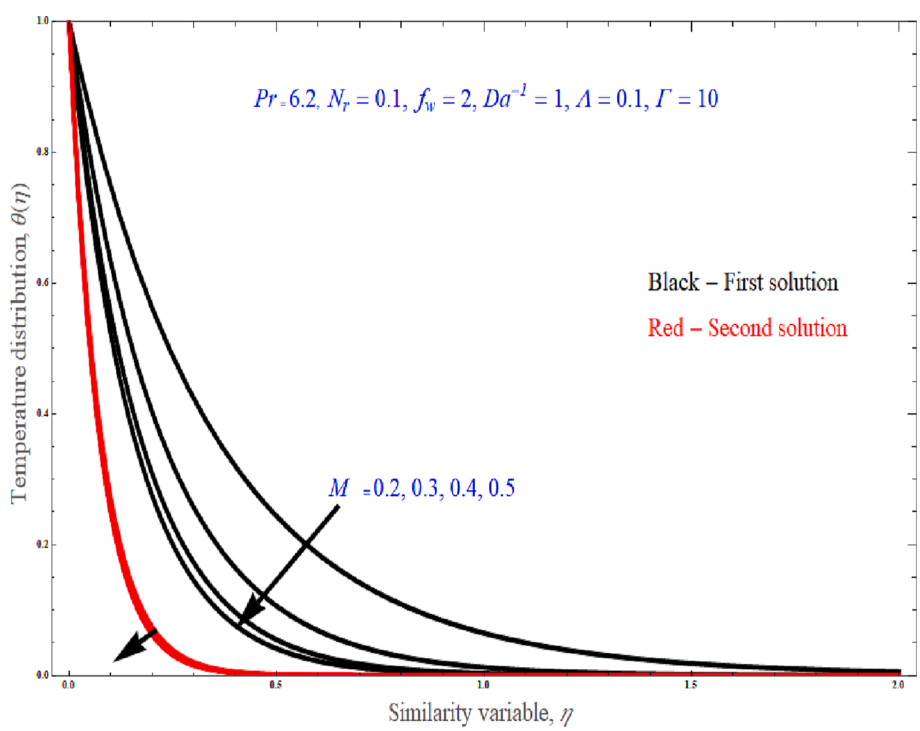

Fig. 5. An impact of M on temperature profile.

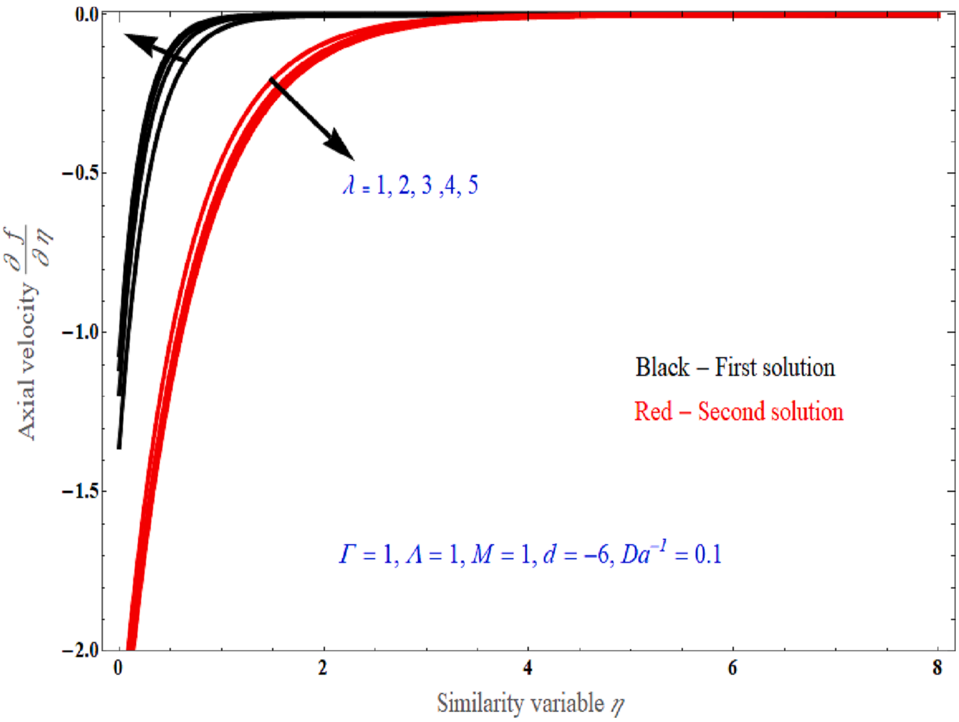

Fig. 6. An impact of λ on velocity profile.

Additionally, it is evident from the aforementioned different roots, we acquire the results to the current problem.

3.1. Analytical solution for temperature equation

Now, in order to get the exact solutions to equation (13), we introduced a new variable $t = \frac{Pr}{\delta^2} e^{-\delta\eta}$, consequently, using the new variable in equation (13) and exposing it to boundary condition (14) produces the desired result:

$$t\frac{d^2\theta}{dt^2} + (m + nt)\frac{d\theta}{dt} = 0, \tag{22}$$

where.

$$m = 1 - \frac{3Prf_w}{\delta(1 + Nr)} - \frac{3Prd}{\delta^2(1 + \Gamma\delta)(1 + Nr)}, \quad n = \frac{3Prd}{(1 + \Gamma\delta)(1 + Nr)}.$$

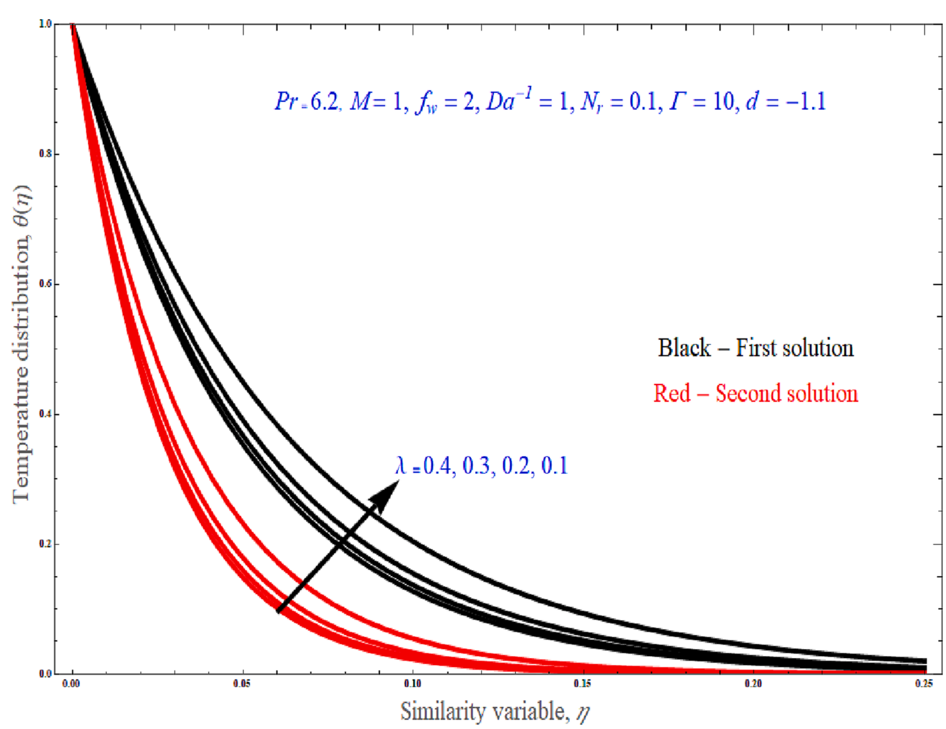

Fig. 7. An impact λ on temperature profile.

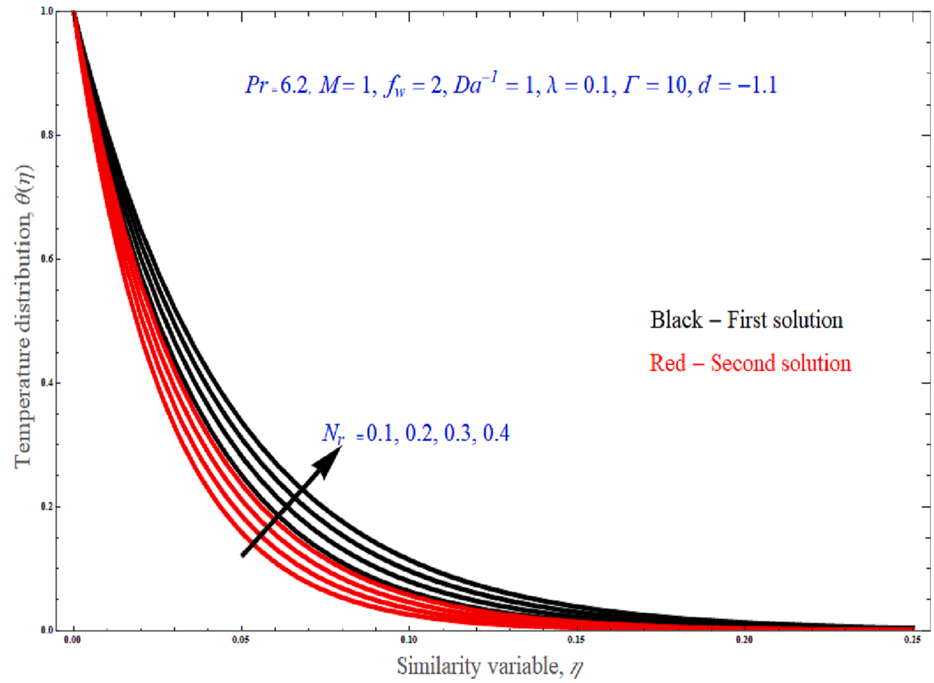

Fig. 8. An impact of N_r on temperature profile.

in addition to boundary constraints are.

$$\theta\left(\frac{Pr}{\delta^2}\right) = 1, \quad \text{and} \quad \theta(0) = 0. \tag{23}$$

Integrating equation (22) can be directly twice, we have.

$$\theta(t) = \frac{c_1}{n^{1-m}} \int_0^{nt} \sigma^{a-1} e^{-\sigma} d\sigma + c_2, \tag{24}$$

herec_1 and c_2 , which are constant being estimated later, simply imposing barrier constraints to equation (24). i.e. $\theta\left(\frac{Pr}{\delta^2}\right) = 1$, and $\theta(0) = 0$, the value of constants given as.

$$c_1 = \frac{n^{1-m}}{\Gamma\left(1-m, \frac{nPr}{\alpha^2}\right) - \Gamma(1-m, 0)}, \tag{25}$$

$$c_2 = -\frac{\Gamma(1-m, 0)}{\Gamma\left(1-m, \frac{nPr}{\alpha^2}\right) - \Gamma(1-m, 0)}, \tag{26}$$

Consequently, the results related to equation (22), that obeys boundary restrictions (23) in favor of incomplete gamma function $\Gamma(a, x)$ are follows:

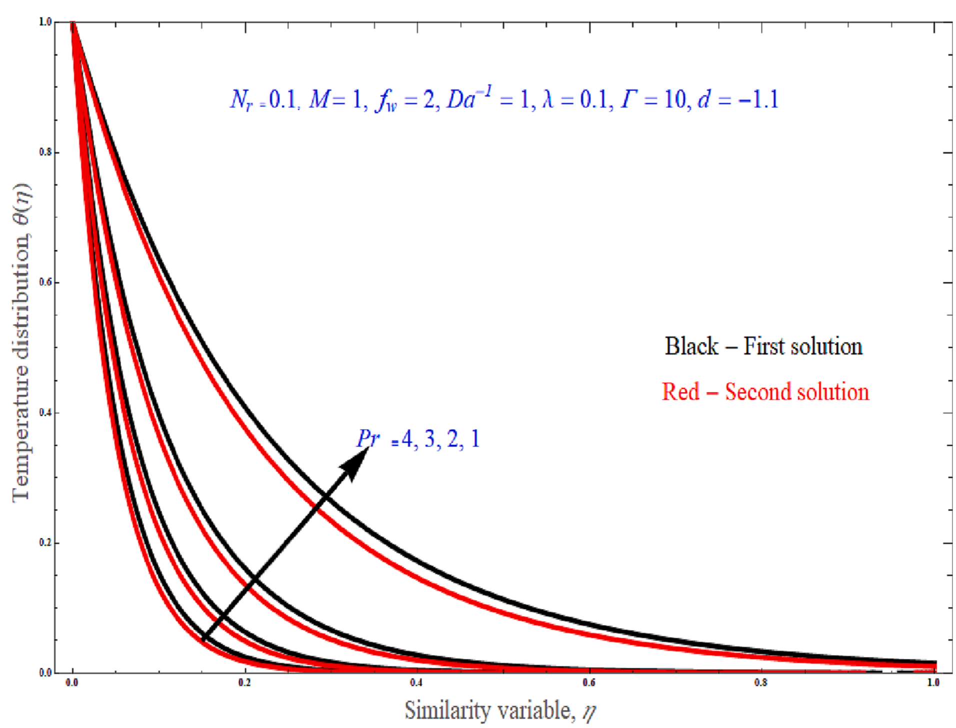

Fig. 9. Prandtl number effects on temperature profile.

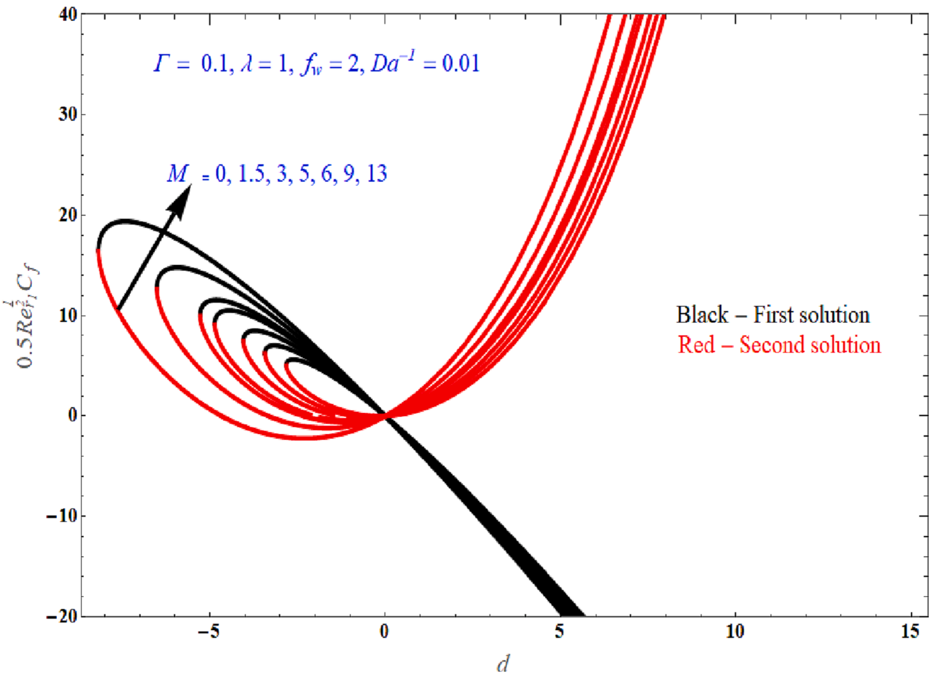

Fig. 10. An impact of M on$0.5Re_{r_1}^{\frac{1}{2}}C_f$.

$$\theta(\eta) = \frac{\Gamma(1-m,0) - \Gamma\left(1-m, \frac{nPr}{\delta^2}e^{-\delta\eta}\right)}{\Gamma(1-m,0) - \Gamma\left(1-m, \frac{nPr}{\delta^2}\right)}, \tag{27}$$

Now, computing the first differentiation of equation (25) with reference to the fictitious variable η resulting into.

$$\frac{d\theta}{d\eta} = \frac{(-3)^{1-m}\left(-\frac{nPr}{\delta^2}e^{-\delta\eta}\right)\delta\left(\frac{nPr}{\delta^2}e^{-\delta\eta}\right)^{1-m}}{\Gamma(1-m,0) - \Gamma\left(1-m, \frac{nPr}{\delta^2}\right)}. \tag{28}$$

In this section, it was established that using the incomplete gamma function as a problem-solving technique delivers a simplified set of unique characteristics, whereas using the alternative ways results in the formation of more complicated special functions. Next, we move on to the findings of the present study.

4. Outcomes of the problem

This research looks at the flow and heat transfer of Casson fluid past a porous shrinking/stretched sheet in two dimensions. Navier slip together with radiation impacts is also discussed in the current article. While employing a similarity conversion, the system of equations is simplified to collection of non-linear ODEs. We have investigated how to comprehend and analyse the graphical shown upper and lower branches

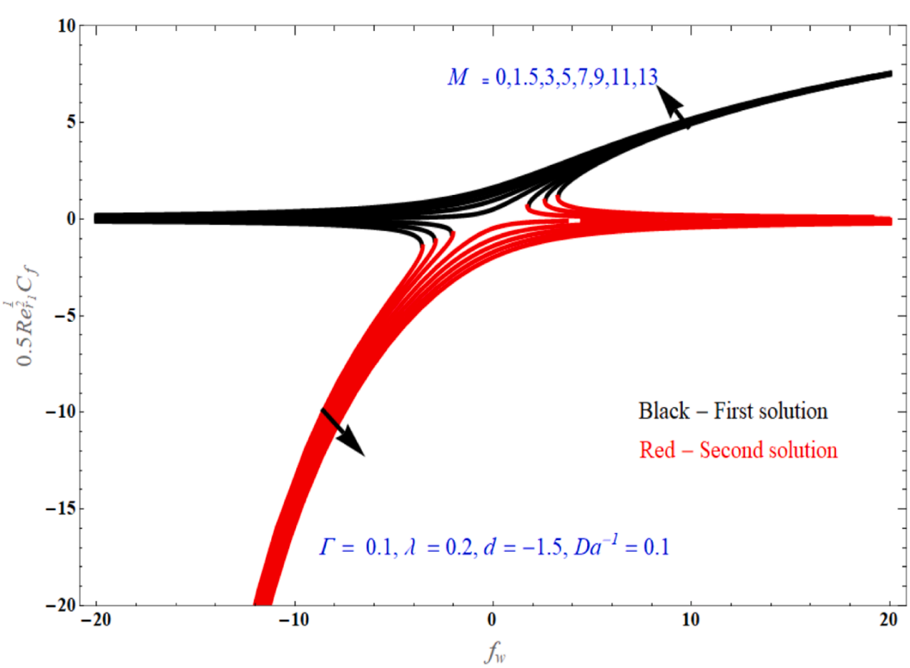

Fig. 11. An impact of M on$0.5Re_{r_1}^{\frac{1}{2}}C_f$.

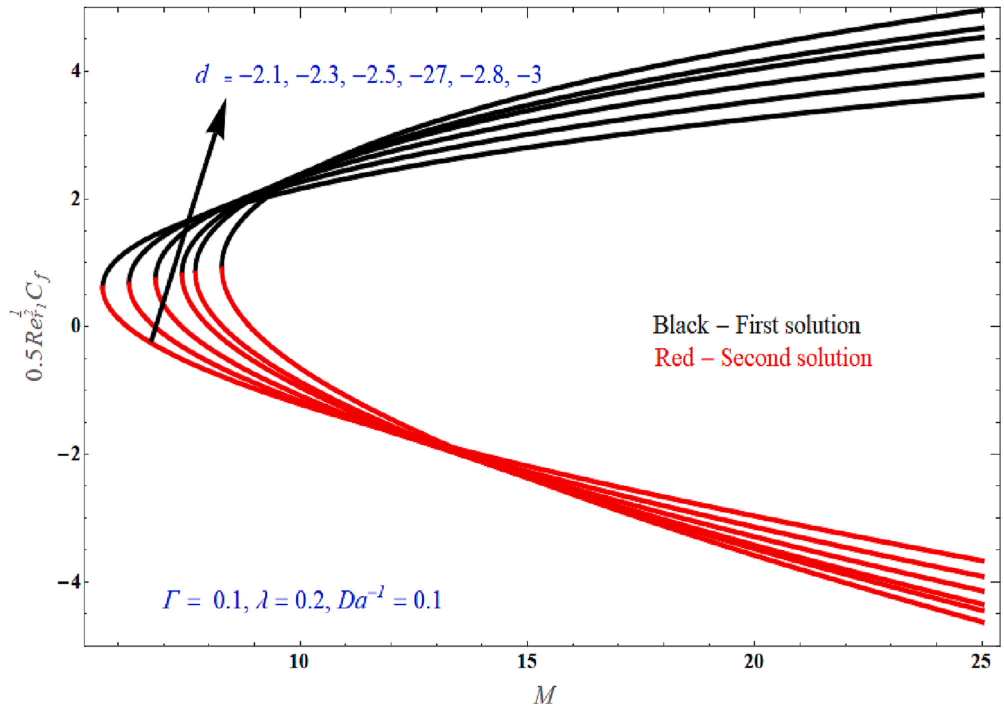

Fig. 12. An impact of Stretching/Shrinking parameter on$0.5Re_{r_1}^{\frac{1}{2}}C_f$.

responses to the casson fluid closed-form analytical solutions to this problem. We have portrayed the significant influences of the pertinent physical factors like, magnetic field, Mass suction/injection, N_r and Casson factors on momentum, temperature, with shear stress profile.

The consequences of f_w upon momentum and temperature distributions are demonstrated in Figs. 2-3, correspondingly. Findings suggested momentum anticipated beyond upper branch solution enhances (first solution) with greater mass suction/injection value, while lower branch solution (second solution) displays the reverse phenomenon. Alternatively, larger mass suction/injection value creates a reduction in thermal later, especially seen in lower and upper branch solutions. Justification for aforementioned features are that the liquid closer to layer is sucked up more quickly. since a higher value of mass suction/injection value, contributing to a greater velocity. Additionally, temperature drops as a result of extracting more intensely heated fluid via porous surface.

Figs. 4-5, respectively, indicate the changes in momentum and temperature distribution as a function of$M$. It is clear from looking at the

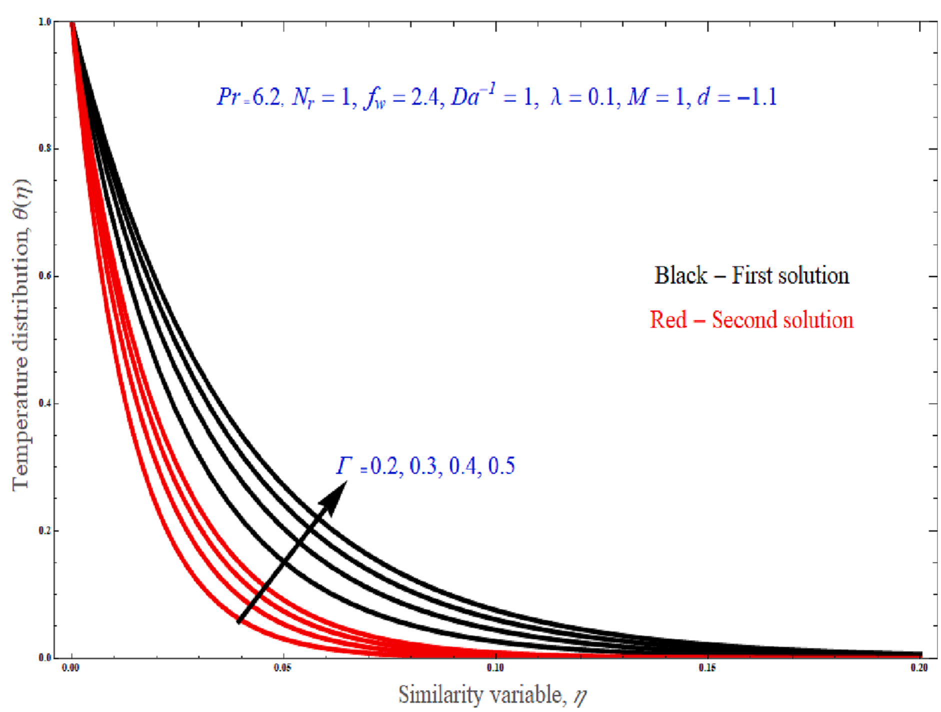

Fig. 13. An impact of Γ on temperature profile.

Table1
Comparison of present study and related works by other authors.

Related works by other uuthors	Fluids	Value of α
Crane 1970 [59]	Newtonian	$\alpha=1$
Pavlov 1974 [60]	Newtonian	$\alpha=\sqrt{1+M}$
Umair [57]	Non-Newtonian	$f(\eta)=f_w+\frac{\lambda}{\beta_a}(1-\exp[-\beta_a\eta])$, $\beta_a=\frac{3f_w\left(\frac{\rho_{hnf}}{\rho_f}\right)\pm\sqrt{9f_w^2\left(\frac{\rho_{hnf}}{\rho_f}\right)^2+4\left(\frac{\mu_{hnf}}{\mu_f}\right)3\lambda\left(\frac{\rho_{hnf}}{\rho_f}\right)+\left(\frac{\sigma_{hnf}}{\sigma_f}\right)M}}{2\left(\frac{\mu_{hnf}}{\mu_f}\right)}$,
Present work	Non-Newtonian	$F(\eta)=f_w+\frac{d}{\delta(1+\Gamma\delta)}(1-e^{-\delta\eta})$, $\left(1+\frac{1}{\lambda}\right)\Gamma\delta^3+\left\{\left(1+\frac{1}{\lambda}\right)-3f_w\Gamma\right\}\delta^2-$ $(3f_w+\Gamma Da^{-1}+M\Gamma)\delta-(3d+Da^{-1}+M)=0$,

upper branch solution that the increase in M causes the velocity to increase with a decreasing temperature profile. Unfortunately, the second solution branch implements the opposite outcome. Since the magnetic field has a significant impact on fluid flow, raising M allows the velocity to decrease. Consequently, the fluid temperature decreases with larger$M$.

Figs. 6-7 demonstrate the impact of λ over momentum and temperature distribution. In both Profile of the fluid momentum and temperature decreases as quantity of λ increases in second solution branch. Because of development of λ, the fluid gets more viscous. Consequently, greater resistance is provided, resulting in a thinner momentum and temperature boundary surface in both upper and lower solution branch. It can clearly be examined that the momentum distribution profiles are increases as the slip parameter are increasing and momentum boundary layer thickness increases in first solution.

Fig. 8 shows the temperature profile for different values ofN_r. The temperature behaves uniquely in both the upper and lower branch solution. The first and second branch solution increases with the increasing value of theN_r. From a physical point of view, the impact of the superior values of the radiation parameter progresses the thermal conductivity which can create amplification in the temperature as well as in thermal boundary layer thickness.

Fig. 9 scrutinized the relationship between the Prandtl number and the temperature distribution. We can see from the curve that as the Prandtl increases slightly, the thickness of the temperature boundary layer diminishes in both solution branches.

Fig. 10 presents two solutions for the skin friction factor by changing M in terms of the value for stretched or contracting. If d is minimized, the coefficient of skin friction grows. Momentum gradients at the surface develop as the surface is extended or shrunk more quickly, respectively. Consequently, as d drops, the skin friction improves. But on the other hand, the skin friction factor rises with M because of fluid velocity will expand with a stronger magnetic factor. Additionally, the threshold for the occurrence of dual solutions rises as M. Fig. 11 presents dual solutions versus f_w taking M variations into account. The coefficient of skin friction reduces with reducing suction parameter but increases with increasing injection strength for a constant M, according to a physically valid upper branch solution. The skin friction coefficient appears to be zero for an injection velocity that is quite high. In contrast, it rapidly rises as suction velocity increases. Similarly, shear stress is elevated by M values that are larger. The development of the skin friction factor with respect to mass suction/injection, in which suction enhances the momentum differences over the surface as well as injection lessens it.

Fig. 12 exhibits the deviations of d about lower and upper solution branches over magnetic field parameter for skin friction factor. According to the observations, there are multiple solutions available only in the scenario of the diminishing parameter. Furthermore, the greater value of the shrinking parameter enhances both streams solutions of skin friction factor. This typically occurs because the fluid flow or velocity patterns are diminished with increasing values of the shrinking factor, and so as a result, the velocity as well as skin friction obey the rule of inversion proportionality. Consequently, as a result for this interpretation, necessary the skin friction factor increases.

Fig. 13 shows the shrinking / stretching of a surface as a function of temperature. Additionally, the value of slip parameter Γ grows as the border layer does in both instances of upper and lower branch solution.

5. Concluding remarks

During this investigation, we closely investigate the flow and heat transfer characteristics of non-Newtonian magnetohydrodynamic axisymmetric fluid over a stretching/shrinking sheet with the effect of thermal radiation, mass suction/injection, including Navier slip condition. After adopting a suitable similarity transformation to represent the velocity and temperature equations as a set of ODEs, after that are cracked analytically. In the situation of flow across a sheet that is contracting /stretching, a specific closed form analytical solution is found. pertinent bodily characteristics, such as mass suction/injection, Magnetic parameter, casson parameter, radiation and prandtl number has been studied in the present problem. The following observations can be made from the current investigation:

- For the shrinking sheet case, only a dual solution is obtained.
- When f_w is enhanced, the first branch velocity profile improves, but the second branch behaviour is the inverse, and both branches temperatures fall.
- Increases in momentum and lowered temperature profile are caused by the magnetic parameter.
- The consequences of Pr on temperature and the width of the thermal boundary is diametrically opposed.
- Radiation will rise in temperature distributions by expanding the thermal boundary layer width.
- The skin friction coefficient increases for increasing with$M$.

A limiting example of the present study is established by many previous works, as follows:

- In the presence of hybrid nanofluid, and absence of porous medium {our results}→{results of Khan [57].
- In the absence of MHD, the results of the problem showed that the electrical conductivity of base fluid is so small.

In future, we plan to perform a similar investigation on non-Newtonian fluids and a different fluid with the effect of slip condition in a porous medium.

5.1. Validation

The temperature behavior of the present problem is verified with the closed-form analytical solution proposed by Crane (1970). Furthermore, in the absence of radiation and viscous dissipation, the results of the problem for heat sink yield the results of the analogous isothermal problem for species concentration. Table 1 shows related works by other authors and finding existing results.

Declaration of Competing Interest

The authors declare that they have no known competing financial interests or personal relationships that could have appeared to influence the work reported in this paper.

Data availability

No data was used for the research described in the article.

Acknowledgments

L.M.P. acknowledges partial financial support from ANID through *Convocatoria Nacional Subvención a Instalación en la Academia Convocatoria Año 2021*, Grant SA77210040. Also, Dr. U.S. Mahabaleshwar is thankful to Professor Dr. David Laroze, Director of the High Research Institute University of Tarapaca 1520 Antofagasta Street, Box 7D, Arica, Chile for his hospitality during his stay at the University of Tarapaca.

References

[1] O. Abdulaziz, N.F.M. Noor, I. Hashim, Homotopy analysis method for fully developed MHD micropolar fluid flow between vertical porous plates, Int. J. Numer. Methods Eng. 78 (2009) 817–827.
[2] S. Srinivas, R. Muthuraj, Effects of thermal radiation and space porosity on MHD mixed convection flow in a vertical channel using homotopy analysis method, Commun. Nonlinear Sci. Numer. Simulat. 15 (8) (2010) 2098–2108.
[3] J.K. Zhang, B.W. Li, Y.Y. Chen, Hall effects on natural convection of participating MHD with thermal radiation in a cavity, Int. J. Heat Mass Transf. 66 (2013) 838–843.
[4] M.M. Ali, A.A. Mamun, M.A. Maleque, N.H.M.A. Azim, Radiation effects on MHD free convection flow along vertical flat plate in presence of joule heating and heat generation, Procedia Eng. 56 (2013).
[5] B.C. Sakiadis, Boundary-layer behavior on continuous solid surfaces: i. boundary-layer equations for two-dimensional and axisymmetric flow, J. Am. Institute Chem. Eng. 7 (2) (1961) 221–225.
[6] B.C. Sakiadis, Boundary-layer behavior on continuous solid surfaces: III. the boundary layer on a continuous cylindrical surface, J. Am. Institute Chem. Eng. 7 (3) (1961) 467–472.
[7] L.J. Crane, Flow past a stretching plate, Zeitschrift für angewandte Mathematik und Physik ZAMP. 21 (4) (1970) 645–647.
[8] M. Miklavcic, C.Y. Wang, Viscous flow due to a shrinking sheet, Q. Appl. Math. 64 (2006) 283–290.
[9] C.Y. Wang, Stagnation flow towards a shrinking sheet, Int. J. Non Linear Mech. 43 (2008) 377–382.
[10] T. Fang, S. Yao, J. Zhang, A. Aziz, Viscous flow over a shrinking sheet with a second order slip flow model, Commun. Nonlinear Sci. Numer. Simulat. 15 (2010) 1831–1842.
[11] K. Zaimi, A. Ishak, I. Pop, Boundary layer flow and heat transfer past a permeable shrinking sheet in a nanofluid with radiation effect, Adv. Mech. Eng. (2012, 2012,) 1–7.
[12] U.S. Mahabaleshwar, K.R. Nagaraju, M.A. Sheremet, Effect of Mass Transfer and MHD Induced Navier's Slip Flow Due to a non Linear Stretching Sheet, J. Eng. Thermophys. 28 (2019) 578–590.
[13] U.S. Mahabaleshwar, I.E. Sarris, G. Lorenzini, Effect of radiation and Navier slip boundary of Walter's liquid B flow over a stretching sheet in a porous media, Int. J. Heat Mass Transf. 127 (2018) 1327–1337.
[14] T. Anusha, U.S. Mahabaleshwar, M. Hatami, Navier slip effect on the thermal-flow of Walters' liquid B flow due to porous stretching/shrinking with heat and mass transfer, Case Stud. Therm. Eng. 28 (2021), 101691.
[15] M. Khan, M. Rahman, Flow and heat transfer to modified second grade fluid over a non-linear stretching sheet, AIP Adv. 5 (2015), 087157.
[16] M. Rahman, M. Manzur, M. Khan, Mixed convection heat transfer to modified second grade fluid in the presence of thermal, J. Mol. Liq. 223 (2016) 217–223.
[17] P.D. Ariel, Axisymmetric flow due to a stretching sheet with partial slip, Int. J. Comput. Math. Appl. 54 (2007) 1169–1183.
[18] M. Sajid, T. Hayat, S. Asghar, K. Vajravelu, Analytic solution for axisymmetric flow over a nonlinearly stretching sheet, Arch. Appl. Mech. 78 (2008) 127–134.
[19] U.S. Mahabaleshwar, K.R. Nagaraju, P.N.V. Kumar, N.A. Kelson, An MHD Navier's slip flow over axisymmetric linear stretching sheet using differential transform method, Int. J. Appl. Comput. Math. 4 (30) (2018) 1–13.
[20] F.A. Soomro, A. Zaib, R.U. Haq, M. Sheikholeslami, Dual nature solution of water functionalized copper nanoparticles along a permeable shrinking cylinder: FDM approach, Int. J. Heat Mass Transf. 129 (2019) 1242–1249.
[21] Z. Abbas, M. Sheikh, S.S. Motsa, Numerical solution of binary chemical reaction on stagnation point flow of Casson fluid over a stretching/shrinking sheet with thermal radiation, Energy 95 (2016) 12–20.
[22] M.F. Javed, M.I. Khan, N.B. Khan, R. Muhammad, M. Ur, S.W. Rehman, T.A. K. Khan, Axisymmetric flow of Casson fluid by a swirling cylinder, Results Phys. 9 (2018) 1250–1255.
[23] J. Raza, Thermal radiation and slip effects on magnetohydrodynamic(MHD) stagnation point flow of Casson fluid over a convective stretching sheet, Propul. Power Res. 18 (2019) 138–146.
[24] R.K. Dash, K.N. Mehta, Casson fluid flow in a pipe filled with a homogeneous porous medium, Int. J. Eng. Sci. 34 (1996) 1145e56.
[25] M.H. Abolbashari, N. Freidoonimehr, F. Nazari, M.M. Rashidi, Analytical modeling of entropy generation for Casson nanofluid flow induced by a stretching surface, Adv. Powder Technol. 26 (2015) 542e52.
[26] U.S. Mahabaleshwar, E.H. Aly, T. Anusha, MHD slip flow of a Casson hybrid nanofluid over a stretching/shrinking sheet with thermal radiation, Chin. J. Phys.. 80 (2022) 74–106.
[27] T. Anusha, Huang-Nan Huang, U.S. Mahabaleshwar, Two dimensional unsteady stagnation point flow of Casson hybrid nanofluid over a permeable flat surface and heat transfer analysis with radiation. J. Taiwan Instit. Chem. Eng. 127 (2021), 79-91.
[28] M. Turkyilmazoglu, Heat and flow across a rotating disc due to a constant horizontal magnetic field, Z. Naturforsch. 77 (2022) 329–337.
[29] M. Turkyilmazoglu, Heat and mass transfer on the MHD fluid flow due to a porous rotating disk with hall current and variable properties, J. Heat Transfer 133 (2011), 021701.
[30] M. Turkyilmazoglu, Algebraic solutions of flow and heat for some nanofluids over deformable and permeable surfaces, Int. J. Numer. Meth. Heat Fluid Flow 27 (2017) 2259–2267.
[31] N.S. Anuar, N. Bachok, M. Turkyilmazoglu, N.M. Arifin, H. Rosali, Analytical and stability analysis of MHD flow past a nonlinearly deforming vertical surface in carbon nanotubes, Alex. Eng. J. 59 (2020) 497–507.
[32] N.S. Wahid, N.M. Arifin, M. Turkyilmazoglu, M.E.H. Hafidzuddin, N.A.A. Rahmin, MHD Hybrid Cu-Al2O3/Water Nanofluid Flow with Thermal Radiation and Partial Slip Past a Permeable Stretching Surface: Analytical Solution, J. Nano Res. 64 (2020) 75–91.
[33] B. Jalili, A. Mousavi, P. Jalili, A. Shateri, D.D. Ganji, Thermal analysis of fluid flow with heat generation for different logarithmic surfaces, Int. J. Eng. 35 (2022) 2291–2296.
[34] P. Jalili, B. Jalili, A. Shateri, D.D. Ganji, A novel fractional analytical technique for the time-space fractional equations appearing in oil pollution, Int. J. Eng. 35 (2022) 2386–2394.
[35] B. Jalili, P. Jalili, A. Shateri, D.D. Ganji, Rigid plate submerged in a Newtonian fluid and fraction differential equation problem via Caputo fractional derivative, Partial Differential Equations Appl. Mathematics. 6 (2022), 100452.
[36] B. Jalili, S. Sadighi, P. Jalili, D.D. Ganji, Characteristic of ferrofluid flow over a stretching sheet with suction with injection, Case Stud. Therm. Eng. 14 (2019), 100470.
[37] B. Jalili, A.D. Ganji, S.S. Nourazar, D.D. Ganji, Thermal analysis of williamson fluid flow with Lorentz force on the stretching sheet, Case Stud. Therm. Eng. 39 (2022), 102374.
[38] P. Jalili, H. Narimisa, B. Jalili, A. Shateri, D.D. Ganji, A novel analytical approach to micropolar nanofluid thermal analysis in the presence of thermophoresis, Brownian motion, and Hall currents, Soft. Comput. 27 (2023) 677–689.
[39] B. Jalili, P. Jalili, S. Sadighi, D.D. Ganji, Effect of magnetic and boundary parameters on flow characteristics analysis of micropolar ferrofluid through the shrinking sheet with effective thermal conductivity, Chin. J. Phys. 71 (2021) 136–150.
[40] P. Jalili, K. Kazerani, B. Jalili, D.D. Ganji, Investigation of thermal analysis and pressure drop in non-continuous helical baffle with different helix angles and hybrid nanoparticles, Case Stud. Therm. Eng. 36 (2022), 102209.
[41] M. Hassan, F.M. Oudina, A. Faisal, A. Ghafar, A.I. Ismail, Thermal energy and mass tra sport of shear thinning fluid under effects of low to high shear rate viscosity, Int. J. Thermofluids. 15 (2022), 100176.
[42] U. Khan, F.M. Oudina, A. Zaib, A. Ishak, S.A. Bakar, E.S.M. Sherif, D. Baleanu, An exact solution of a Casson fluid flow induced by dust particles with hybrid nanofluid over a stretching sheet subject to Lorentz forces, Waves Random Complex Media (2022), https://doi.org/10.1080/17455030.2022.2102689.
[43] J. Raza, F.M. Oudina, L.A. Lund, The flow of magnetized convective Casson liquid via a porous channel with shrinking and stationary walls, Pramana-J. Phys. 96 (2022) 229.
[44] F.M. Oudina, Numerical modelling of the hydrodynamic stability in vertical annulus with heat source of different lengths, Emerg. Sci. Technol. Int. J. 20 (2017) 1324–1333.
[45] F.M. Oudina, Convective heat transfer of titania nanofluids of different base fluids in cylindrical annulus with discrete heat source, Heat Transfer. 48 (2019) 135–147.
[46] Y.D. Reddy, F.M. Oudina, B.S. Goud, A.I. Ismail, Radiation, velocity, and thermal slips effect toward MHD boundary layer flow through heat and mass transport of Williamson nanofluid with porous medium, Arab. J. Sci. Eng. 47 (2022) 16355–16369.

[47] A. Shafiq, F.M. Oudina, T.N. Sindhu, G. Rasool, Sensitivity analysis for Walters-B nanoliquid flow over a radiative Riga surface by RSM, Scientia Iranica B. 29 (2022) 1236–1249.

[48] K. Dhif, F.M. Oudina, S. Chouf, H. Vaidya, A.J. Chamkha, Journal of Nanofluids. 10 (2021) 616–626.

[49] P. Jalili, A.A. Azar, B. Jalili, Z. Asadi, D.D. Ganji, Heat transfer analysis in cylindrical polar system with magnetic field: A novel hybrid analytical and Numerical technique, Case Stud. Therm. Eng. 40 (2022), 102524.

[50] J. Prakash, P.D. Prasad, G.V. Kumar, R. Kumar, S.V.K. Varma, Heat and Mass Transfer Hydromagnetic Radiative Casson fluid flow over an Exponentially Stretching sheet with heat source/sink, Int. J. Eng. Sci. 5 (2016), 12-23.

[51] P.K. Kameswaran, S. Shaw, P. Sibanda, Dual solution of Casson fluid flow over a stretching or shrinking sheet, Sadhana 39 (2014) 1573–1583.

[52] U.S. Mahabaleshwar, E.H. Aly, T. Anusha, MHD slip flow of casson hybrid nanofluid over a stretching/shrinking sheet with thermal radiation, Chin. J. Phys. 80 (2022) 74–106.

[53] U.S. Mahabaleshwar, T. Maranna, F. Sofos, Analytical investigation of an incompressible viscous laminar Casson fluid flow past a stretching/shrinking sheet, Sci. Rep.. 12 (2022) 18404.

[54] A.B. Vishalakshi, T. Maranna, U.S. Mahabaleshwar, D. Laroze, An Effect of MHD on Non-Newtonian Fluid Flow over a Porous Stretching/Shrinking Sheet with Heat Transfer. Applied Sciences. 12 (2022), 4937.

[55] T. Maranna, K.N. Sneha, U.S. Mahabaleshwar, I.E. Sarris, T.E. Karakasidis, An effect of radiation and MHD Newtonian fluid flow over a stretching/shrinking sheet with CNTs and mass transpiration, Appl. Sci. 12 (2022) 5466.

[56] M. Darzi, M. Vatani, S.E. Ghasemi, et al., Effect of thermal radiation on velocity and temperature fields of a thin liquid film over a stretching sheet in a porous medium, Eur. Phys. J. Plus. 130 (2015) 100.

[57] U. Khan, A. Zaib, A. Ishak, N.C. Roy, S.A. Bakar, T. Muhammad, A.H.A. Aty, I. S. Yahia, Exact solutions for MHD axisymmetric hybrid nanofluid flow and heat transfer over a permeable non-linear radially shrinking/stretching surface with mutual impacts of thermal radiation, Eur. Phys. J. Special Topics. 231 (2022) 1195–1204.

[58] M. Nawaz, R. Naz, M. Awais, Magnetohydrodynamic axisymmetric flow of casson fluid with variable thermal conductivity and free stream, Alex. Eng. J. 57 (2018) 2043–2050.

[59] L.J. Crane, Flow past a stretching plate, Z. Angew. Math. Phys. 21 (1970) 645–647.

[60] K.B. Pavlov, magnetohydrodynamic flow of incompressible viscous fluid caused by of a surface. M. Gidrodinamika. 4(1974), 146-147.